Behavioural Brain Research 436 (2023) 114074

Contents lists available at ScienceDirect

Behavioural Brain Research

journal homepage: www.elsevier.com/locate/bbr

Research report

Individual-specific characterization of event-related hemodynamic responses during an auditory task: An exploratory study

J. McLinden [a], S.B. Borgheai [a], S. Hosni [a], C. Kumar [b], N. Rahimi [b], M. Shao [b], K.M. Spencer [c], Y. Shahriari [a,*]

[a] Department of Electrical, Computer, and Biomedical Engineering, University of Rhode Island, Kingston, RI, USA
[b] Department of Computer and Information Science, University of Massachusetts Dartmouth, MA, USA
[c] Department of Psychiatry, VA Boston Healthcare System and Harvard Medical School, Jamaica Plain, Boston, MA, USA

ARTICLE INFO

Keywords:
Functional near-infrared spectroscopy (fNIRS)
Auditory processing
Feature extraction
Independent component analysis (ICA)

ABSTRACT

Functional near-infrared spectroscopy (fNIRS) has been established as an informative modality for understanding the hemodynamic-metabolic correlates of cortical auditory processing. To date, such knowledge has shown broad clinical applications in the diagnosis, treatment, and intervention procedures in disorders affecting auditory processing; however, exploration of the hemodynamic response to auditory tasks is yet incomplete. This holds particularly true in the context of auditory event-related fNIRS experiments, where preliminary work has shown the presence of valid responses while leaving the need for more comprehensive explorations of the hemodynamic correlates of event-related auditory processing. In this study, we apply an individual-specific approach to characterize fNIRS-based hemodynamic changes during an auditory task in healthy adults. Oxygenated hemoglobin (HbO_2) concentration change time courses were acquired from eight participants. Independent component analysis (ICA) was then applied to isolate individual-specific class discriminative spatial filters, which were then applied to HbO_2 time courses to extract auditory-related hemodynamic features. While six of eight participants produced significant class discriminative features before ICA-based spatial filtering, the proposed method identified significant auditory hemodynamic features in all participants. Furthermore, ICA-based filtering improved correlation between trial labels and extracted features in every participant. For the first time, this study demonstrates hemodynamic features important in experiments exploring auditory processing as well as the utility of individual-specific ICA-based spatial filtering in fNIRS-based feature extraction techniques in auditory experiments. These outcomes provide insights for future studies exploring auditory hemodynamic characteristics and may eventually provide a baseline framework for better understanding auditory response dysfunctions in clinical populations.

1. Introduction

Capturing the cortical correlates of auditory processing has improved the understanding of the mechanisms of normal auditory processing [1–3] and altered cortical processing in a number of conditions, including dyslexia [4,5], schizophrenia [6,7], central auditory processing disorder [8], and autism spectrum disorder [9,10]. Such information can be used alongside traditional outcome measurements to evaluate drug interventions [11] and inform potential therapeutic neurofeedback strategies [12]. Cortical correlates of auditory processing have also been employed to assess outcomes in individuals with cochlear implants [13] and could potentially facilitate the diagnosis of attention deficit hyperactivity disorder (ADHD) [14]. The value of cortical auditory neuromarkers is underscored by the breadth of potential clinical applications and relevance to many conditions that affect auditory processing. To date, various types of neuroimaging techniques have been employed to advance the understanding of normal and disrupted cortical auditory processing activity [3,15]. Although functional magnetic resonance imaging (fMRI) has been one of the most utilized neuroimaging tools to observe the metabolic correlates of auditory processing [16–20], functional near-infrared spectroscopy (fNIRS) has shown promise as an alternative modality that provides distinct advantages over fMRI, especially in auditory experimentation contexts due to its low auditory noise levels produced during recording [3]. Although

* Corresponding author.
E-mail address: yalda_shahriari@uri.edu (Y. Shahriari).

https://doi.org/10.1016/j.bbr.2022.114074
Received 4 March 2022; Received in revised form 11 August 2022; Accepted 21 August 2022
Available online 24 August 2022

techniques such as sparse sampling [16] have been proposed to partially mitigate the effects of auditory machine noise in fMRI, all solutions thus far constrain experimental design [17]. fNIRS neuroimaging technology can be especially beneficial for auditory experimental setups as it allows for flexible and naturalistic experimental designs [21] in addition to its portability, low cost, and decent compromise it offers between temporal and spatial resolution [22]. This optical technology, which measures concentration changes of oxygenated (HbO_2) and deoxygenated (HbR) hemoglobin in cerebral blood flow, provides an indirect measurement of neural activity by reflecting the metabolic needs of local neuron populations [23] important for auditory processing exploration.

Despite distinct advantages of fNIRS over and synergies between this neuroimaging modality with existing modalities, limited fNIRS auditory processing research has been conducted. Tian et al. (2021) determined that sound localization information was encoded in hemodynamic responses by classifying features extracted from oxygenated hemoglobin time series signals [24]. Shader et al. (2021) also determined significant activations of the left and right auditory cortices in response to auditory-only speech stimuli, spatially differentiating these responses from visual-only speech stimuli [25]. Additionally, Santosa et al. (2014) demonstrated that hemodynamic responses are lateralized to the right hemisphere while listening to music relative to noise, even when music was presented in the presence of noise [26]. Other works have also demonstrated the feasibility of classifying hemodynamic responses by the type of auditory stimuli presented [27,28]. In addition to the characterization of normal auditory processing, fNIRS has applications in characterizing pathological auditory processing conditions. For example, Issa et al. (2016) found that hemodynamic activity was increased in auditory and non-auditory regions in individuals with tinnitus when compared to healthy controls [29]. Bell et al. (2020) explored speech comprehension in children with hearing aids when compared with normally-hearing controls [30].

To date, fNIRS responses in auditory tasks have been characterized in both block design [31–33] and event-related design [34,35] paradigms. Event-related experiments have often been disregarded in favor of block design experiments; however, it has been demonstrated that event related experimental designs can elicit valid hemodynamic responses while retaining the flexibility that this experimental design approach offers [36]. For example, Ehlis et al. (2009) employed an auditory event related paradigm to explore hemodynamic correlates of sensory gating and their relationships with simultaneously recorded electroencephalography (EEG), determining a significant positive correlation between the hemodynamic response and sensory gating [35]. Mushtaq et al. (2019) found significant activation over the superior temporal cortex in response to speech and speech-like stimuli in normally-hearing children ages 6–12 [37]. Kennan et al. (2002) reported an event-related response in an auditory oddball task consisting of a series of standard tones with rare presentation of a deviant tone. In this study, the authors characterized the hemodynamic response to the stimulus as a peak in total hemoglobin concentration (HbT) with a peak latency of 5.8 s and 5.9 s duration measured as full width at half maximum [34]. The results of this study are based on group epoch averages, but do not account for inter-individual variability or trial level features.

The existing body of fMRI auditory processing literature provides additional insights to our understanding of the metabolic correlates of auditory processing. Frühholz et al. (2020) were able to characterize infra-slow oscillations evoked by socially relevant verbal auditory stimuli, determining that both simple and complex auditory stimuli produce both a transient and a sustained blood oxygen level-dependent (BOLD) response [18]. BOLD response magnitude to simple auditory stimuli have also been shown to correlate with loudness percept [19,32]. Significant group differences were found between schizophrenia patients and matched healthy control participants in an auditory oddball task that were not present in a visual oddball task [20], further demonstrating the need for greater understanding of the hemodynamic correlates of event-related auditory processing.

Hemodynamic responses to various tasks, including motor imagery, hybrid visual oddball/mental arithmetic tasks, and tasks designed to invoke auditory processing [38–40], have demonstrated significant inter-individual variability [38,41,42], demonstrating the necessity of individual-specific feature extraction techniques sensitive to individual differences in hemodynamic response waveform characteristics. Determining class discriminative features in auditory oddball tasks would be beneficial for further understanding the role of cerebral hemodynamics in auditory processing, and characterizing the metabolic correlates of neural auditory processing impairments such as tinnitus [40,43], acquired brain injury [44], and schizophrenia [45]. In the latter case, developing an understanding of the hemodynamic correlates of auditory processing could inform promising neurofeedback techniques to mitigate verbal auditory hallucinations [12,46] and provide additional insight to characterize neural abnormalities in auditory processing in schizophrenic populations [15,47,48]. Characterizing auditory task-related hemodynamic changes could also further inform the development of fNIRS-based brain-computer interfaces (BCIs) as well as hybrid BCIs incorporating fNIRS with other modalities, such as EEG [38,39].

fNIRS feature extraction strategies can be confounded by physiological noise sources including Mayer waves, respiration, and heart rate [49,50]. To this effect, several methods have been suggested for denoising and subsequent extraction of task-relevant information, including the common average reference (CAR) [24,51], independent component analysis (ICA) [51–54], short-channel regression [55], and methods based on principal component analysis (PCA) [56,57]. Of these methods, ICA, which decomposes signal time courses measured across multiple channels into components representative of mutually independent sources [58], stands out as a unique data-driven denoising approach with potential feature extraction applications by separating neural task-related activity from physiological noise and other noise sources. ICA can also incorporate information from other sensors to improve noise removal by including more direct measures of noise sources, such as accelerometer readings of head motion [59], and also has been used in fNIRS to extract task-related components from multichannel recordings [60]. In addition, ICA has demonstrated to be able to separate components containing hemodynamic responses from noise components, further demonstrating its promise as both a de-noising and feature extraction approach [54]. However, it should be noted that ICA-based approaches that rely on manual retention of task-related components can fail to remove physiological noise associated with the task, and methods that rely on applying ICA using only long-distance channels are insufficient to fully characterize the cortical hemodynamic response [61].

Despite previous work establishing the promise and viability of auditory oddball experiments, more work must be done to characterize healthy individuals' task-related hemodynamic changes induced by auditory oddball tasks before its utility in patient populations can be fully explored. The most relevant study to date using fNIRS as a signal acquisition method was performed by Kennan et al. (2002), which established the presence of an auditory oddball response in the total hemoglobin concentration change time courses in five healthy individuals and characterized some features common among participants, but did not characterize individual differences between participants [34].

This study aims to characterize individual-specific class discriminative hemodynamic features in an event-related auditory task in a healthy population by recording participants' task-related hemodynamic changes induced by deviant stimuli over several regions of interest in auditory tasks. We propose an ICA-based method to determine class discriminative components in an event-related auditory task. Characterization of auditory task-related changes in the hemodynamic time series would contribute to the underexplored field of auditory processing research using fNIRS. The outcomes from this study intend to add novel information to the existing sparse fNIRS auditory event-related

literature base as a step towards the application of such experimental paradigms to future experimental protocols including healthy participants and eventually clinical populations suffering from auditory response dysfunctions.

2. Methods

2.1. Participants, experimental protocol, and signal acquisition

Eight healthy participants (three female, mean age 29.25 ± 10.07 years) with no known history of neurological or auditory processing disorder were recruited from the University of Rhode Island. This study was approved by the institutional review board (IRB) of the University of Rhode Island, and all participants provided informed consent before participation in the study.

Participants were seated in a comfortable chair before a cap was placed on their heads. Cap position was determined using measurements relative to anatomical landmarks, with Cz positioned at the midpoints between the inion and nasion and between both ears, in accordance with the international 10–20 system. fNIRS optodes were placed according to the montage shown in Fig. 1 to cover the Frontal (F), Left Auditory (LA), and Right Auditory (RA) regions of interest (ROIs). The optode locations were selected using the fOLD toolbox [62]. A pair of headphones (Sony Group Corporation) were placed over the ears of the participant before calibration of the fNIRS system.

Participants completed six experimental runs of an auditory oddball task. Each run consisted of 20 deviant stimuli and a randomized number of standard stimuli (average 122 standard stimuli per run). The final two deviant epochs and the associated preceding standard epochs were removed from further analysis due to the presence of motion artifacts in a number of participants, retaining 108 (6 runs x 18 deviant stimuli/run = 108) deviant epochs and an average of 648 (6 runs x 108 standard stimuli/run = 648) standard epochs per participant. Standard stimuli were 1 kHz tones with 500 ms duration and deviant stimuli were 40 Hz white noise click trains with 500 ms duration. Stimuli were presented with a 2 s inter-stimulus interval (ISI). Between five and seven standard stimuli were presented at random between subsequent deviant stimuli, guaranteeing a period of 15–20 s between subsequent deviant stimulus presentations. A diagram of the proposed experimental protocol is presented in Fig. 1. Participants were instructed to count the number of deviant stimuli heard in each run while ignoring standard stimuli. Additionally, upon hearing the n^{th} deviant stimulus in the run, participants were asked to mentally count up from n to n + 4 in order to increase the attentional load of the task, as active auditory oddball tasks have been shown to activate attention-related networks that are otherwise not activated in passive auditory oddball tasks [63]. During this period of mental counting, participants were instructed to imagine the sound of the enunciation of the numbers during counting. This was intended to include an auditory imagery component to the task shown to involve attention and semantic processing networks [64]. Participants were instructed to avoid any changes in respiratory pattern related to the task to reduce potential respiratory artifacts in the hemodynamic signal. Hemodynamic data were acquired using a NIRScout (NIRx Inc.) system at a sampling rate of 7.81 Hz from 7 sources and 8 detectors over a total of 14 channels spread across three regions of interest (ROIs) indicated as F, LA, and RA.(Fig. 2).

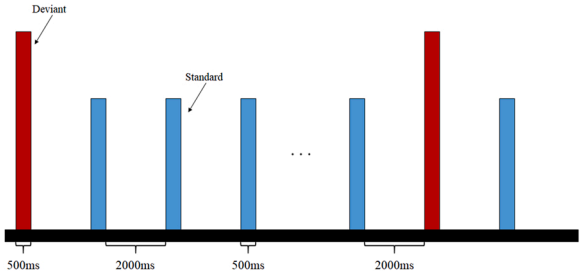

Fig. 1. A diagram of the proposed experimental design: Red bars indicate deviant stimuli and blue bars represent standard stimuli. The spaces between stimuli represent the inter-stimulus interval. Stimulus presentation order is randomized to create an auditory oddball task and reduce phase synchrony between deviant stimulus presentation and unrelated physiological activity. The first five stimuli following a deviant stimulus are standard, guaranteeing at least 15 s between previous deviant stimulus onset and current deviant stimulus onset. A following deviant stimulus may come directly after the first five stimuli following the previous deviant stimulus, or there may be one or two additional standard stimuli before the following deviant stimulus is presented, corresponding to a maximum delay of 20 s between previous deviant stimulus onset and following deviant stimulus onset.

2.2. Signal analysis

Optical density signals were bandpass filtered 0.005–0.7 Hz and converted to oxygenated and deoxygenated hemoglobin concentration changes (HbO_2 and HbR, respectively) using the modified Beer-Lambert Law in the nirsLab software package (NIRx Inc.). This passband was selected to remove heartbeat artifacts (~1 Hz) but retain the frequency bands shown to contain both known artifacts such as Mayer waves (~0.1 Hz) and respiration artifacts (~0.2–0.5 Hz) and possible task-related information, as well as several cycles of the largest possible period of deviant stimulus presentation (18 s) [65]. Subsequent analyses were performed on HbO_2 signals using the MATLAB software package (The MathWorks, Inc.). HbO_2 was selected as previous work has suggested that features extracted from HbO_2 exhibit greater reproducibility both spatially and temporally in event-related fNIRS experiments [66], though the analysis was repeated for the HbR time series. These results are available in Appendix A. ICA was then applied to the HbO_2 signals using the infomax algorithm, generating 14 statistically independent components. These components were epoched 0–20 s relative to stimulus onset. 5 s sliding windows were extracted from each component epoch ranging from 0 to 5 s, 2–7 s, 4–9 s, 6–11 s, 8–13 s, and 10–15 s relative to stimulus onset, and signal slope was extracted via linear regression within each window. Signal slope was selected from a set of

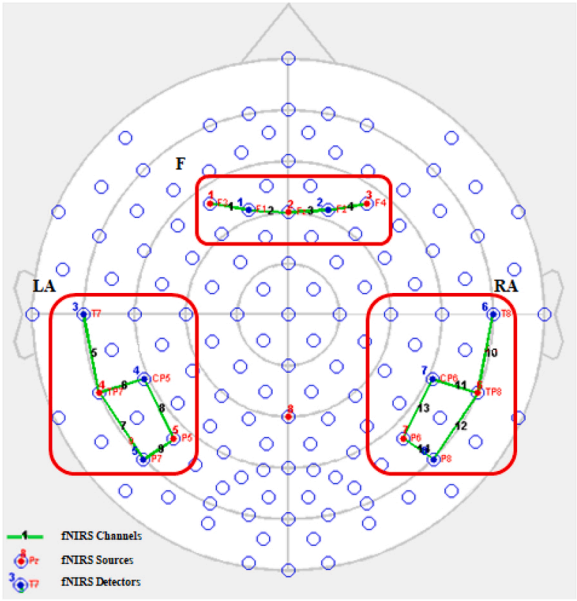

Fig. 2. The experimental montage utilized in this study. Green lines indicate fNIRS channels, red dots indicate fNIRS sources, and blue dots indicate fNIRS detectors. Different regions of interest are grouped by a red box and labeled. The regions were selected to cover the frontal (F), left auditory (LA), and right auditory (RA) regions.

explored features successfully employed in other task discrimination studies (maximum, minimum, skewness, kurtosis, slope) [65,67,68] for this analysis after it was determined that this feature produced the most robust outcomes. Specifically, slope was the only explored feature that demonstrated Spearman correlation (ρ) between features and trial labels (deviant and standard) with $p < 0.01$ in over half the participants. Spearman correlation calculated between trial labels and extracted features was used to evaluate the relationship between hemodynamic signal slope and the trial labels. All participants but one (S07) produced multiple components with features that correlated well with trial labels. For these participants, components containing a feature from any time window that correlated with the trial labels with a *p*-value of less than 0.01 were retained, while all other components were rejected. This threshold was selected based upon visual inspection of a subset of the components meeting this criterion across the participant pool. However, for participant S07, these criteria were relaxed to include components containing a feature that correlates with trial labels in at least one window with a *p*-value of less than 0.05 as only one component contained a feature that met the original inclusion criteria, greatly reducing the spatially discriminative information contained in the backprojected data. Retained components were then projected back into the channel-time space, and slope features were again extracted from the epoched hemodynamic signal using the same 5 s sliding window (0–5 s, 2–7 s, 4–9 s, 6–11 s, 8–13 s, and 10–15 s). Features were then averaged channel-wise over each region of interest and Spearman correlation was calculated between each averaged feature by region and trial label. The correlation analysis therefore represents the difference in signal slope time-locked to stimulus onset between deviant and standard stimuli where a positive ρ-value indicates increased slope in the corresponding time window in deviant trials relative to slope observed in that window time-locked to standard stimulus onset. All *p*-values were subjected to Bonferroni correction to determine statistical significance, producing an adjusted α level of 0.0028 (3 ROIs x 6 windows). Epochs were also extracted from the original signal and ICA-filtered signal − 5–20 s relative to stimulus onset and averaged by stimulus type to observe characteristics of the signal time series.

3. Results

Fig. 3 shows fourteen component topographies taken from the inverse weight matrix estimated using ICA and the corresponding spectra of each component time course from a representative participant (S01). As it is seen, component spectra are mostly dominated by activity at ~0.1 Hz, suggesting that some physiological noise is retained in most independent components, even those that contain class discriminative information. Additionally, the first components are relatively global, while subsequent components become more spatially localized, suggesting that components accounting for most of the variance in the signal capture global activity commonly associated with noise.

Before ICA spatial filtering, six of eight participants demonstrated significant correlation between extracted slope and trial labels (S01, S02, S04, S05, S06, S08). Of these participants, five participants demonstrated significant correlation between features and trial labels in the frontal region (S01, S04, S05, S06, S08), whereas significant correlation between features and trial labels was observed in the LA regions of three participants (S01, S02, S04, S08) and the RA region of four participants (S01, S02, S04, S08). After applying ICA spatial filtering, all eight participants demonstrated significant correlation between slope in at least one window and region and trial labels. Among these, significant correlation between features and trial labels was observed in the frontal region of six participants (S01, S03, S04, S06, S07, S08), the LA region of all eight participants, and the RA region of six participants (S01, S02, S03, S04, S05, S06). Correlation maps for each participant are shown in Appendix A.

Feature correlation maps and average HbO_2 signals from the same representative participant (S01) are also displayed in Fig. 4. As it is seen in Fig. 4 (bottom), a short negative deflection precedes a longer period of positive slope, which is then followed by a similar period of negative slope (Fig. 4 bottom). The overall shape of the response is retained after ICA spatial filtering, though slightly altered due to removal of the non-class discriminative components. The correlation maps displayed in Fig. 4 (top) reflect these observations, as a period of significant positive correlation between signal slope and trial labels in the 4–9 s window is followed by a period of significant negative correlation between signal

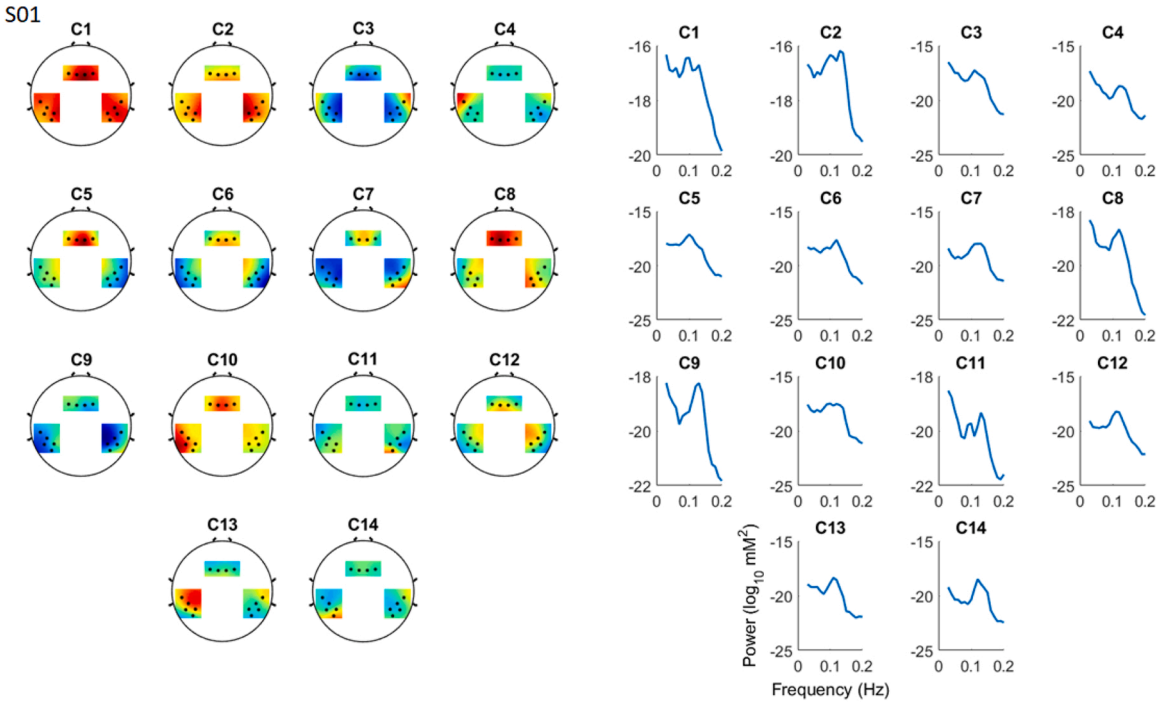

Fig. 3. Left: Fourteen component topographies (C1 to C14) from a representative participant (S01) shown in arbitrary units (au). Right: Power spectra from the same representative participant for all 14 components.

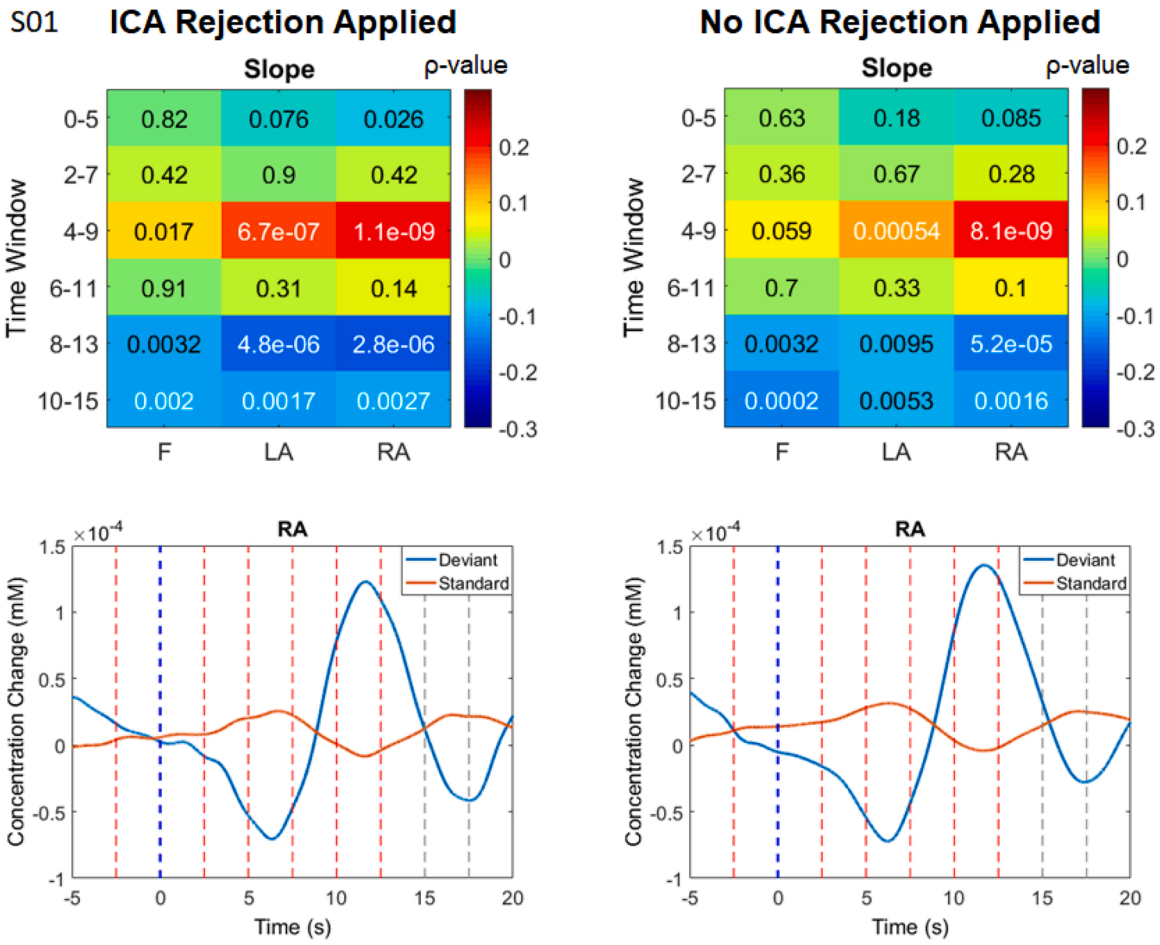

Fig. 4. Top: Comparison of correlations between trial labels and features between the backprojected HbO_2 waveform after ICA spatial filtering and the original waveform after ICA spatial filtering from a representative participant (S01)–note: in this case, five independent components were retained. Significant corrected *p*-values ($p < 0.0028$) are displayed in white, while non-significant *p*-values are displayed in black. Deeper red corresponds with positive correlation while deeper blue corresponds with negative correlation. Bottom: Comparison of HbO_2 waveforms averaged over the RA region after and before ICA-based spatial filtering applied. Deviant stimulus onset is plotted with a blue dashed line, while standard stimulus onset is plotted with a red dashed line. Gray dashed lines represent stimulus onset that could be either deviant or standard.

slope and trial labels in the 8–13 s and 10–15 s windows. This basic pattern is somewhat retained in most other participants' responses, as six of eight participants (S01, S03, S04, S06, S07, S08) demonstrate significant positive correlation between signal slope and trial labels in the three earlier time windows (0–5 s, 2–7 s, 4–9 s). However, responses broadly differ between participants spatially and temporally, with maximal signal slope correlation occurring in either earlier or later time windows (windows ranging from 0 to 5 s and 8–13 s). Notably, S05 produces a shorter period of positive slope followed by a much more pronounced period of negative slope, which was extracted as a feature that significantly correlates with trial labels, though there is no preceding period of significant positive correlation. Additionally, S06 demonstrates periodic oscillatory behavior, and the major periods of slope changes (early negative, middle positive, late positive) are extracted as significant features. All participants' average responses and correlation maps are available in Appendix A.

Fig. 5 displays the highest absolute value Spearman correlation (ρ) observed in each region for each participant before and after ICA spatial filtering. As shown, the proposed ICA spatial filtering method increased the highest observed ρ in all participants and in almost every region. The most pronounced improvements in correlation between extracted features and trial labels is observed in participants with the fewest components retained, such as S03 and S07 (two and three components retained, respectively), indicating that noise is distributed differently between components across participants. Marginal improvements were found in other participants; however, the consistency of improvement in correlation was notable as this occurred in all participants (only four instances of ρ decreasing in a given region were observed).

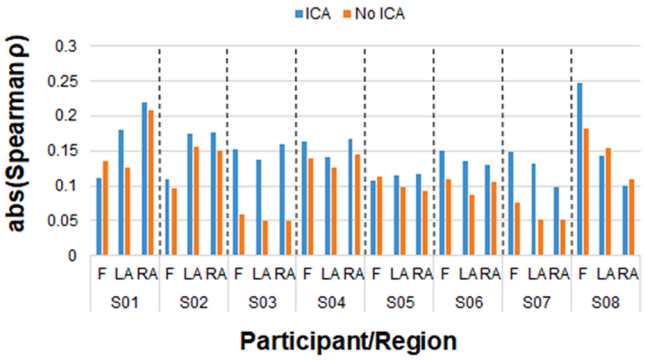

Fig. 5. Comparison of the highest absolute value Spearman correlation (ρ) values by region and preprocessing scheme (ICA vs. No ICA) for the HbO_2 results of each participant. Participants are separated by a dotted line.

4. Discussion

In this study, task-related hemodynamic changes during an event-related auditory task were characterized across healthy individuals. The outcomes can provide insight to the growing field of fNIRS-based auditory experiments by characterizing the task-related changes in hemodynamic activity during auditory processing through the demonstration of statistically significant changes in signal slope following deviant stimulus presentation relative to standard stimulus presentation. Our study further demonstrated improvement in the discriminative feature set using an ICA-based denoising strategy to retain task-related components and reject unrelated components. While previous work has characterized the hemodynamic auditory oddball response measured by fNIRS [34], we propose a feature extraction scheme using ICA-based spatial filtering that was shown to extract class discriminative features sensitive to individual differences in the response waveform. Overall, we found that signal slope significantly correlated with trial labels in most participants before ICA spatial filtering. All participants demonstrated significant correlation between trial labels and extracted features after ICA spatial filtering. We further demonstrated the importance of individual-specific feature extraction strategies to characterize hemodynamic changes related to auditory tasks. Sensitivity to individual differences in response waveforms has shown to be beneficial to the analysis of hemodynamic signals. For example, Hosni et al. (2020) and Borgheai et al. (2020) both demonstrated the benefits of using individual-specific hemodynamic features when developing hybrid EEG-fNIRS BCIs for patients with amyotrophic lateral sclerosis (ALS) [38,39]. Additionally, Holper et al. (2011) demonstrated significant inter-individual variability in the hemodynamic responses of healthy participants during a motor imagery task [42]. Here, we demonstrate important inter-individual variability both temporally and spatially in the hemodynamic signal changes induced by deviant auditory stimuli, reflecting findings in other paradigms and emphasizing the need for either individual-specific approaches or analyses robust to differences in hemodynamic patterns across participants.

While our work also demonstrated the value of ICA as a feature extraction strategy in the context of fNIRS-based auditory experiments, ICA-based feature extraction techniques have been effectively employed in other fNIRS studies by other groups. For example, Akgül et al. used ICA to decompose hemodynamic signals recorded during a visual oddball paradigm and components were retained based on correlation with a hemodynamic response signal template [60]. Katura et al. applied a similar ICA-based strategy during a finger-tapping task, selecting class-related components using mean inter-trial cross-correlation as a metric to select class-related ICA components. This approach provides the distinct advantage of forgoing the use of a predefined hemodynamic response function (HRF), allowing for more flexibility when analyzing responses that may vary across participants [69]. We adopt a similar approach, using Spearman correlation between features extracted from component time series and trial labels to determine class discriminative components. We additionally project the retained components back into channel space in order to retain spatial information in further analyses, subsequently improving the interpretability of our results. Interestingly, this approach considerably improved correlation between features and trial labels in all our participants. The most remarkable improvements were observed in participants where fewer components were retained, specifically, S03 and S07. Systemic oscillatory activity was observed in these participants, as evidenced by the intense activity at ~0.1 Hz in multiple components (see Appendix A), suggesting that the current approach is capable of extracting features of the hemodynamic response from individuals that exhibit large systemic artifacts. Considering the fact that activity at the ~0.1 Hz frequency range is associated with the Mayer wave, which are oscillations caused by arterial blood pressure changes [70], the observed large systemic artifacts observed in these participants may be the likely cause of this phenomenon. It is noted that the spectral power of Mayer wave artifacts can negatively impact the ability to estimate the hemodynamic response, as demonstrated by Yücel et al. [71].

The auditory paradigm employed in this study evoked significant bilateral changes in signal slope in six of eight participants after ICA-based spatial filtering. Six of eight participants also demonstrated significant correlation between features extracted from the frontal region and trial labels. A possible explanation for this observation is the relative proximity of the frontal optodes to the prefrontal region, where oddball responses are found in event-related potentials [72]. Indeed, the mental counting task employed to ensure participant attention has been shown to activate the prefrontal region [68], possibly explaining the presence of significant attention-related features near this region. The additional observation of bilateral activation of the auditory cortex using fNIRS in auditory oddball tasks is previously unreported, as the hemodynamic auditory oddball response was only characterized in the left auditory cortex using fNIRS in the preceding work [34]. However, this observation has some precedence as previous studies using fNIRS have demonstrated significant bilateral activation of the auditory cortex in response to simple auditory stimuli in block design paradigms [31,73]. Bilateral auditory cortex activation was also observed in auditory oddball studies conducted using fMRI techniques [20,74]. However, two participants did not exhibit significant bilateral features, and instead produced significant features only in the LA region. A possible explanation of the lack of right auditory activation in these participants is the role of the right auditory cortex in pitch detection [75]. While the pitches of each stimulus type are different, the change in pitch between deviant and standard tones is only one of several contextual differences between the tones. Further work should be conducted to quantify the possible hemodynamic response associated with the previously characterized electrical response to such stimuli. This would improve understanding of the current results and aid in understanding the steady-state auditory response usually produced by such a stimulus by including hemodynamic signal components and the previously characterized increase in evoked power at auditory stimulation frequency [15]. To date, several studies have demonstrated the importance of cerebral hemodynamic activity associated with auditory processing in multiple clinical domains. While auditory fNIRS studies have found success in cases where this modality provides distinct advantages over other neuroimaging modalities, the characterization of hemodynamic responses to auditory stimuli in healthy adults contributes to the expanding literature base exploring more general problems and clinical populations. For example, fNIRS has been used to characterize altered cortical activity in individuals with tinnitus, including increased oxygenated hemoglobin consumption in the auditory cortex and other regions [29] and altered functional connectivity in a population with tinnitus when compared to a group of healthy controls in both auditory and non-auditory regions during an auditory processing task [76]. Differences between healthy controls and schizophrenia patients were also explored using fMRI in an auditory oddball task by Collier et al. (2016), who found more significant differences in auditory attention tasks than in visual attention between these two populations [20]. These studies provide evidence supporting the clinical value of measuring cerebral vascular-hemodynamics in individuals engaged in auditory processing tasks. Most notably, fNIRS has been successfully employed in characterizing plasticity in the auditory cortex in individuals with cochlear implants [77,78]. This modality is particularly suited to exploring auditory cortex neuroplasticity due to its compatibility with the implants, which is not shared with most other neuroimaging approaches, including fMRI [79]. fNIRS has also been used in auditory processing studies with young children owing to the modality's tolerability and relative resistance to motion artifacts [80].

There are several limitations to the conclusions drawn by this study. This study was performed with a limited number of participants, limiting statistical power, and the breadth of potential inter-individual variability in task-related hemodynamics may not be fully characterized. However, the purpose of this study was to apply an exploratory

individual-specific analysis approach to extract features characterizing the task-related components of the hemodynamic signal during an auditory task in healthy participants. The results presented demonstrate the inter-individual variability inherent to the hemodynamic response measured by fNIRS and highlight the need for analysis approaches capable of accounting for this variability. While we were successful in exploring this inter-individual variability, further exploration is warranted to characterize population-level hemodynamic responses to auditory tasks. Additionally, the limited number of optodes may influence the ability of the employed noise reduction techniques to reduce or eliminate global noise components. Although ICA has been demonstrated to improve signal quality in similar low-density fNIRS montages [54], further work should be conducted that employs either sufficient optode coverage to characterize and remove global noise or short-channel recordings to remove systemic artifacts, including physiological noise related to the task [81], which currently may not be completely removed using the current ICA spatial filtering approach [82]. As such, this crucial step is necessary to ascertain that the features extracted purely reflect cortical hemodynamic changes. Other potential hemodynamic features could be explored, such as signal mean, slope, peak, minimum, maximum, skewness, kurtosis [83], or β-values from a generalized linear model (GLM) [84] to better characterize distinctive hemodynamic features. Of these potential features to explore, the GLM approach is most crucial due to the widespread adoption of these features in the literature base characterizing the hemodynamic response [85]. However, this study demonstrates significant differences in signal slope in response to deviant stimuli when compared to standard stimuli in an auditory oddball task in all participants using the window selected, suggesting that in many cases, this feature extraction approach can capture important task related hemodynamic information in these tasks. More research should also be done to thoroughly characterize the discriminative responses in healthy and pathological populations, informing further pathological biomarkers applicable in diagnostic techniques. The characterization of the hemodynamic waveform related to the present task also has potential closed-loop BCI applications. Closed-loop BCIs that rely on auditory stimuli have particular applications to individuals in the late stages of ALS, where participants become locked-in to the point of losing voluntary eye gaze control [86]. Future work exploring the possibility of the extension of this paradigm to a closed-loop BCI application is warranted. As another future direction, fNIRS can also be recorded concurrently with EEG, providing additional insights into neural functions and responses to established EEG paradigms that have been foundational in auditory processing research [35]. Further multimodal exploration of these responses could expand the understanding of compound neural dynamics and help to characterize abnormal cortical patterns, as well as providing insights to neuromodulation approaches such as transcranial direct current stimulation (tDCS), which has shown promise in interventional procedures involving patients with auditory processing dysfunctions [87].

CRediT authorship contribution statement

John McLinden: Methodology, Investigation, Formal analysis, Software, Writing – original draft, Visualization. **S. Bahram Borgheai:** Methodology, Writing – review & editing. **Sarah Ismail Hosni:** Methodology, Writing – review and editing **Chetan Kumar:** Writing – review & editing. **Neela Rahimi:** Writing – review & editing. **Ming Shao:** Writing – review & editing, Funding acquisition. **Kevin Spencer:** Conceptualization, Methodology, Writing – review & editing, Funding acquisition. **Yalda Shahriari:** Conceptualization, Methodology, Writing – review & editing, Project administration, Funding acquisition.

Data Availability

The data that has been used is confidential.

Acknowledgement

This study was supported by the National Science Foundation (NSF-2024418). The authors would like to thank the participants who took part in this study, without whom this study would not have been possible. The authors declare that the research was conducted in the absence of any commercial or financial relationships that could be construed as a potential conflict of interest.

References

[1] K. Teshima, K. Ishida, H. Nittono, Auditory perceptual processing during musical imagery: an event-related potential study, Neurosci. Lett. 762 (2021), 136148, https://doi.org/10.1016/j.neulet.2021.136148.
[2] T. Riggins, L.S. Scott, P300 development from infancy to adolescence, Psychophysiology 57 (2020), e13346, https://doi.org/10.1111/psyp.13346.
[3] L.P.H. van de Rijt, M.M. van Wanrooij, A.F.M. Snik, E.A.M. Mylanus, A.J. van Opstal, A. Roye, Measuring cortical activity during auditory processing with functional near-infrared spectroscopy, J. Hear. Sci. 8 (2018) 9–18, https://doi.org/10.17430/1003278.
[4] C. Gu, H.-Y. Bi, Auditory processing deficit in individuals with dyslexia: a meta-analysis of mismatch negativity, Neurosci. Biobehav. Rev. 116 (2020) 396–405, https://doi.org/10.1016/j.neubiorev.2020.06.032.
[5] J.A. Hämäläinen, H.K. Salminen, P.H.T. Leppänen, Basic auditory processing deficits in dyslexia: systematic review of the behavioral and event-related potential/ field evidence, J. Learn. Disabil. 46 (2013) 413–427, https://doi.org/10.1177/0022219411436213.
[6] Y. Hirano, N. Oribe, T. Onitsuka, S. Kanba, P.G. Nestor, T. Hosokawa, M. Levin, M. E. Shenton, R.W. McCarley, K.M. Spencer, Auditory cortex volume and gamma oscillation abnormalities in Schizophrenia, Clin. EEG Neurosci. 51 (2020) 244–251, https://doi.org/10.1177/1550059420914201.
[7] B.A. Coffman, S.M. Haigh, T.K. Murphy, J. Leiter-Mcbeth, D.F. Salisbury, Reduced auditory segmentation potentials in first-episode schizophrenia, Schizophr. Res. 195 (2018) 421–427, https://doi.org/10.1016/j.schres.2017.10.011.
[8] A. Koravand, B. Jutras, M. Lassonde, Abnormalities in cortical auditory responses in children with central auditory processing disorder, Neuroscience 346 (2017) 135–148, https://doi.org/10.1016/j.neuroscience.2017.01.011.
[9] C. Vlaskamp, B. Oranje, G.F. Madsen, J.R. Møllegaard Jepsen, S. Durston, C. Cantio, B. Glenthøj, N. Bilenberg, Auditory processing in autism spectrum disorder: Mismatch negativity deficits, Autism Res 10 (2017) 1857–1865, https://doi.org/10.1002/aur.1821.
[10] R.A. Seymour, G. Rippon, G. Gooding-Williams, P.F. Sowman, K. Kessler, Reduced auditory steady state responses in autism spectrum disorder, Mol. Autism 11 (2020) 56, https://doi.org/10.1186/s13229-020-00357-y.
[11] D.C. Javitt, K.M. Spencer, G.K. Thaker, G. Winterer, M. Hajós, Neurophysiological biomarkers for drug development in schizophrenia, Nat. Rev. Drug Discov. 7 (2008) 68–83, https://doi.org/10.1038/nrd2463.
[12] H. Storchak, J. Hudak, F.B. Haeussinger, D. Rosenbaum, A.J. Fallgatter, A.-C. Ehlis, Reducing auditory verbal hallucinations by means of fNIRS neurofeedback - a case study with a paranoid schizophrenic patient, Schizophr. Res. 204 (2019) 401–403, https://doi.org/10.1016/j.schres.2018.09.018.
[13] H. Bortfeld, Functional near-infrared spectroscopy as a tool for assessing speech and spoken language processing in pediatric and adult cochlear implant users, Dev. Psychobiol. 61 (2019) 430–443, https://doi.org/10.1002/dev.21818.
[14] J. Byeon, T.Y. Choi, G.H. Won, J. Lee, J.W. Kim, A novel quantitative electroencephalography subtype with high alpha power in ADHD: ADHD or misdiagnosed ADHD, PLoS One 15 (2020), e0242566, https://doi.org/10.1371/journal.pone.0242566.
[15] T.-H. Zhou, N.E. Mueller, K.M. Spencer, S.G. Mallya, K.E. Lewandowski, L. A. Norris, D.L. Levy, B.M. Cohen, D. Öngür, M.-H. Hall, Auditory steady state response deficits are associated with symptom severity and poor functioning in patients with psychotic disorder, Schizophr. Res. 201 (2018) 278–286, https://doi.org/10.1016/j.schres.2018.05.027.
[16] T.M. Talavage, D.A. Hall, How challenges in auditory fMRI led to general advancements for the field, Neuroimage 62 (2012) 641–647, https://doi.org/10.1016/j.neuroimage.2012.01.006.
[17] F. Di Salle, F. Esposito, T. Scarabino, E. Formisano, E. Marciano, C. Saulino, S. Cirillo, R. Elefante, K. Scheffler, E. Seifritz, fMRI of the auditory system: understanding the neural basis of auditory gestalt, Magn. Reson. Imaging 21 (2003) 1213–1224, https://doi.org/10.1016/j.mri.2003.08.023.
[18] S. Frühholz, W. Trost, D. Grandjean, P. Belin, Neural oscillations in human auditory cortex revealed by fast fMRI during auditory perception, Neuroimage 207 (2020), 116401, https://doi.org/10.1016/j.neuroimage.2019.116401.
[19] O. Behler, S. Uppenkamp, Auditory fMRI of sound intensity and loudness for unilateral stimulation, Adv. Exp. Med. Biol. 894 (2016) 165–174, https://doi.org/10.1007/978-3-319-25474-6_18.
[20] A.K. Collier, D.H. Wolf, J.N. Valdez, B.I. Turetsky, M.A. Elliott, R.E. Gur, R.C. Gur, Comparison of auditory and visual oddball fMRI in schizophrenia, Schizophr. Res. 158 (2014) 183–188, https://doi.org/10.1016/j.schres.2014.06.019.
[21] M.A. Rahman, A.B. Siddik, T.K. Ghosh, F. Khanam, M. Ahmad, A narrative review on clinical applications of fNIRS, J. Digit. Imaging 33 (2020) 1167–1184, https://doi.org/10.1007/s10278-020-00387-1.

[22] W.-L. Chen, J. Wagner, N. Heugel, J. Sugar, Y.-W. Lee, L. Conant, M. Malloy, J. Heffernan, B. Quirk, A. Zinos, S.A. Beardsley, R. Prost, H.T. Whelan, Functional near-infrared spectroscopy and its clinical application in the field of neuroscience: advances and future directions, Front. Neurosci. 14 (2020) 724, https://doi.org/10.3389/fnins.2020.00724.
[23] M. Ferrari, V. Quaresima, A brief review on the history of human functional near-infrared spectroscopy (fNIRS) development and fields of application, Neuroimage 63 (2012) 921–935, https://doi.org/10.1016/j.neuroimage.2012.03.049.
[24] X. Tian, Y. Liu, Z. Guo, J. Cai, J. Tang, F. Chen, H. Zhang, Cerebral representation of sound localization using functional near-infrared spectroscopy, Front. Neurosci. 15 (2021), 739706, https://doi.org/10.3389/fnins.2021.739706.
[25] M.J. Shader, R. Luke, N. Gouailhardou, C.M. McKay, The use of broad vs restricted regions of interest in functional near-infrared spectroscopy for measuring cortical activation to auditory-only and visual-only speech, Hear. Res. 406 (2021), 108256, https://doi.org/10.1016/j.heares.2021.108256.
[26] H. Santosa, M.J. Hong, K.-S. Hong, Lateralization of music processing with noises in the auditory cortex: an fNIRS study, Front. Behav. Neurosci. 8 (2014) 418, https://doi.org/10.3389/fnbeh.2014.00418.
[27] K.-S. Hong, H. Santosa, Decoding four different sound-categories in the auditory cortex using functional near-infrared spectroscopy, Hear. Res. 333 (2016) 157–166, https://doi.org/10.1016/j.heares.2016.01.009.
[28] S.-H. Yoo, H. Santosa, C.-S. Kim, K.-S. Hong, Decoding multiple sound-categories in the auditory cortex by neural networks: an fNIRS study, Front. Hum. Neurosci. 15 (2021), 636191, https://doi.org/10.3389/fnhum.2021.636191.
[29] M. Issa, S. Bisconti, I. Kovelman, P. Kileny, G.J. Basura, Human auditory and adjacent nonauditory cerebral cortices are hypermetabolic in tinnitus as measured by functional near-infrared spectroscopy (fNIRS, Neural Plast. 2016 (2016), 7453149, https://doi.org/10.1155/2016/7453149.
[30] L. Bell, Z.E. Peng, F. Pausch, V. Reindl, C. Neuschaefer-Rube, J. Fels, K. Konrad, fNIRS assessment of speech comprehension in children with normal hearing and children with hearing aids in virtual acoustic environments: pilot data and practical recommendations, Child 7 (2020), https://doi.org/10.3390/children7110219.
[31] R. Luke, E. Larson, M.J. Shader, H. Innes-Brown, L. Van Yper, A.K.C. Lee, P. F. Sowman, D. McAlpine, Analysis methods for measuring passive auditory fNIRS responses generated by a block-design paradigm, Neurophotonics 8 (2021) 25008, https://doi.org/10.1117/1.NPh.8.2.025008.
[32] S. Weder, M. Shoushtarian, V. Olivares, X. Zhou, H. Innes-Brown, C. McKay, Cortical fNIRS responses can be better explained by loudness percept than sound intensity, Ear Hear 41 (2020) 1187–1195, https://doi.org/10.1097/AUD.0000000000000836.
[33] L.-C. Chen, P. Sandmann, J.D. Thorne, C.S. Herrmann, S. Debener, Association oF Concurrent fNIRS and EEG signatures in response to auditory and visual stimuli, Brain Topogr. 28 (2015) 710–725, https://doi.org/10.1007/s10548-015-0424-8.
[34] R.P. Kennan, S.G. Horovitz, A. Maki, Y. Yamashita, H. Koizumi, J.C. Gore, Simultaneous recording of event-related auditory oddball response using transcranial near infrared optical topography and surface EEG, Neuroimage 16 (2002) 587–592, https://doi.org/10.1006/nimg.2002.1060.
[35] A.-C. Ehlis, T.M. Ringel, M.M. Plichta, M.M. Richter, M.J. Herrmann, A. J. Fallgatter, Cortical correlates of auditory sensory gating: a simultaneous near-infrared spectroscopy event-related potential study, Neuroscience 159 (2009) 1032–1043, https://doi.org/10.1016/j.neuroscience.2009.01.015.
[36] M.M. Plichta, S. Heinzel, A.-C. Ehlis, P. Pauli, A.J. Fallgatter, Model-based analysis of rapid event-related functional near-infrared spectroscopy (NIRS) data: a parametric validation study, Neuroimage 35 (2007) 625–634, https://doi.org/10.1016/j.neuroimage.2006.11.028.
[37] F. Mushtaq, I.M. Wiggins, P.T. Kitterick, C.A. Anderson, D.E.H. Hartley, Evaluating time-reversed speech and signal-correlated noise as auditory baselines for isolating speech-specific processing using fNIRS, PLoS One 14 (2019), e0219927, https://doi.org/10.1371/journal.pone.0219927.
[38] S.M. Hosni, S.B. Borgheai, J. McLinden, Y. Shahriari, An fNIRS-based motor imagery BCI for ALS: a subject-specific data-driven approach, IEEE Trans. Neural Syst. Rehabil. Eng. 28 (2020) 3063–3073, https://doi.org/10.1109/TNSRE.2020.3038717.
[39] S.B. Borgheai, J. McLinden, A.H. Zisk, S.I. Hosni, R.J. Deligani, M. Abtahi, K. Mankodiya, Y. Shahriari, Enhancing communication for people in late-stage ALS using an fNIRS-based BCI system, IEEE Trans. Neural Syst. Rehabil. Eng. 28 (2020) 1198–1207, https://doi.org/10.1109/TNSRE.2020.2980772.
[40] M. Shoushtarian, R. Alizadehsani, A. Khosravi, N. Acevedo, C.M. McKay, S. Nahavandi, J.B. Fallon, Objective measurement of tinnitus using functional near-infrared spectroscopy and machine learning, PLoS One 15 (2020), e0241695, https://doi.org/10.1371/journal.pone.0241695.
[41] H. Zohdi, F. Scholkmann, U. Wolf, Individual differences in hemodynamic responses measured on the head due to a long-term stimulation involving colored light exposure and a cognitive task: A SPA-fNIRS study, Brain Sci. 11 (2021), https://doi.org/10.3390/brainsci11010054.
[42] L. Holper, D.E. Shalóm, M. Wolf, M. Sigman, Understanding inverse oxygenation responses during motor imagery: a functional near-infrared spectroscopy study, Eur. J. Neurosci. 33 (2011) 2318–2328, https://doi.org/10.1111/j.1460-9568.2011.07720.x.
[43] J.D. San Juan, T. Zhai, A. Ash-Rafzadeh, X.-S. Hu, J. Kim, C. Filipak, K. Guo, M. N. Islam, I. Kovelman, G.J. Basura, Tinnitus and auditory cortex: using adapted functional near-infrared spectroscopy to measure resting-state functional connectivity, Neuroreport 32 (2021) 66–75, https://doi.org/10.1097/WNR.0000000000001561.
[44] E. Jeong, H. Ryu, J.-H. Shin, G.H. Kwon, G. Jo, J.-Y. Lee, High oxygen exchange to music indicates auditory distractibility in acquired brain injury: an fNIRS study with a vector-based phase analysis, Sci. Rep. 8 (2018) 16737, https://doi.org/10.1038/s41598-018-35172-2.
[45] P.-H. Chou, C.-J. Huang, C.-W. Sun, The potential role of functional near-infrared spectroscopy as clinical biomarkers in Schizophrenia, Curr. Pharm. Des. 26 (2020) 201–217, https://doi.org/10.2174/1381612825666191014164511.
[46] Y. Hirano, S. Tamura, Recent findings on neurofeedback training for auditory hallucinations in schizophrenia, Curr. Opin. Psychiatry 34 (2021) 245–252, https://doi.org/10.1097/YCO.0000000000000693.
[47] K.M. Spencer, D.F. Salisbury, M.E. Shenton, R.W. McCarley, Gamma-band auditory steady-state responses are impaired in first episode psychosis, Biol. Psychiatry 64 (2008) 369–375, https://doi.org/10.1016/j.biopsych.2008.02.021.
[48] R.A. Levit, S. Sutton, J. Zubin, Evoked potential correlates of information processing in psychiatric patients, Psychol. Med. 3 (1973) 487–494, https://doi.org/10.1017/s0033291700054295.
[49] G. Bauernfeind, C. Böck, S.C. Wriessnegger, G.R. Müller-Putz, Physiological Noise Removal from fNIRS Signals, Biomed. Tech. (Berl.) 58 (Suppl 1) (2013), https://doi.org/10.1515/bmt-2013-4430.
[50] N.M. Gregg, B.R. White, B.W. Zeff, A.J. Berger, J.P. Culver, Brain specificity of diffuse optical imaging: improvements from superficial signal regression and tomography, Front. Neuroenergetics 2 (2010), https://doi.org/10.3389/fnene.2010.00014.
[51] G. Bauernfeind, S.C. Wriessnegger, I. Daly, G.R. Müller-Putz, Separating heart and brain: on the reduction of physiological noise from multichannel functional near-infrared spectroscopy (fNIRS) signals, J. Neural Eng. 11 (2014) 56010, https://doi.org/10.1088/1741-2560/11/5/056010.
[52] Z. Yuan, Spatiotemporal and time-frequency analysis of functional near infrared spectroscopy brain signals using independent component analysis, J. Biomed. Opt. 18 (2013), 106011, https://doi.org/10.1117/1.JBO.18.10.106011.
[53] S. Kohno, I. Miyai, A. Seiyama, I. Oda, A. Ishikawa, S. Tsuneishi, T. Amita, K. Shimizu, Removal of the skin blood flow artifact in functional near-infrared spectroscopic imaging data through independent component analysis, J. Biomed. Opt. 12 (2007) 62111, https://doi.org/10.1117/1.2814249.
[54] H. Santosa, M.J. Hong, S.-P. Kim, K.-S. Hong, Noise reduction in functional near-infrared spectroscopy signals by independent component analysis, Rev. Sci. Instrum. 84 (2013) 73106, https://doi.org/10.1063/1.4812785.
[55] D. Wyser, M. Mattille, M. Wolf, O. Lambercy, F. Scholkmann, R. Gassert, Short-channel regression in functional near-infrared spectroscopy is more effective when considering heterogeneous scalp hemodynamics, Neurophotonics 7 (2020) 35011, https://doi.org/10.1117/1.NPh.7.3.035011.
[56] X. Zhang, J.A. Noah, J. Hirsch, Separation of the global and local components in functional near-infrared spectroscopy signals using principal component spatial filtering, Neurophotonics 3 (2016) 1–8, https://doi.org/10.1117/1.NPh.3.1.015004.
[57] J. Defenderfer, A. Kerr-German, M. Hedrick, A.T. Buss, Investigating the role of temporal lobe activation in speech perception accuracy with normal hearing adults: An event-related fNIRS study, Neuropsychologia 106 (2017) 31–41, https://doi.org/10.1016/j.neuropsychologia.2017.09.004.
[58] Y. Zhao, P.-P. Sun, F.-L. Tan, X. Hou, C.-Z. Zhu, NIRS-ICA: a MATLAB toolbox for independent component analysis applied in fNIRS studies, Front. Neuroinform. 15 (2021), 683735, https://doi.org/10.3389/fninf.2021.683735.
[59] T. Hiroyasu, Y. Nakamura, H. Yokouchi, Method for removing motion artifacts from fNIRS data using ICA and an acceleration sensor, Annu. Int. Conf. IEEE Eng. Med. Biol. Soc. IEEE Eng. Med. Biol. Soc. Annu. Int. Conf. 2013 (2013) 6800–6803, https://doi.org/10.1109/EMBC.2013.6611118.
[60] C.B. Akgül, A. Akin, B. Sankur, Extraction of cognitive activity-related waveforms from functional near-infrared spectroscopy signals, Med. Biol. Eng. Comput. 44 (2006) 945–958, https://doi.org/10.1007/s11517-006-0116-3.
[61] F. Zhang, D. Cheong, A.F. Khan, Y. Chen, L. Ding, H. Yuan, Correcting physiological noise in whole-head functional near-infrared spectroscopy, J. Neurosci. Methods 360 (2021), 109262, https://doi.org/10.1016/j.jneumeth.2021.109262.
[62] G.A. Zimeo Morais, J.B. Balardin, J.R. Sato, fNIRS optodes' location decider (fOLD): a toolbox for probe arrangement guided by brain regions-of-interest, Sci. Rep. 8 (2018) 3341, https://doi.org/10.1038/s41598-018-21716-z.
[63] C. Justen, C. Herbert, The spatio-temporal dynamics of deviance and target detection in the passive and active auditory oddball paradigm: a sLORETA study, BMC Neurosci. 19 (2018) 25, https://doi.org/10.1186/s12868-018-0422-3.
[64] M. Zvyagintsev, B. Clemens, N. Chechko, K.A. Mathiak, A.T. Sack, K. Mathiak, Brain networks underlying mental imagery of auditory and visual information, Eur. J. Neurosci. 37 (2013) 1421–1434, https://doi.org/10.1111/ejn.12140.
[65] N. Naseer, K.-S. Hong, fNIRS-based brain-computer interfaces: a review, Front. Hum. Neurosci. 9 (2015) 3, https://doi.org/10.3389/fnhum.2015.00003.
[66] M.M. Plichta, M.J. Herrmann, C.G. Baehne, A.-C. Ehlis, M.M. Richter, P. Pauli, A. J. Fallgatter, Event-related functional near-infrared spectroscopy (fNIRS): are the measurements reliable? Neuroimage 31 (2006) 116–124, https://doi.org/10.1016/j.neuroimage.2005.12.008.
[67] E.A. Aydin, Subject-Specific feature selection for near infrared spectroscopy based brain-computer interfaces, Comput. Methods Prog. Biomed. 195 (2020), 105535, https://doi.org/10.1016/j.cmpb.2020.105535.
[68] A. Zafar, K.-S. Hong, Detection and classification of three-class initial dips from prefrontal cortex, Biomed. Opt. Express 8 (2017) 367–383, https://doi.org/10.1364/BOE.8.000367.
[69] T. Katura, H. Sato, Y. Fuchino, T. Yoshida, H. Atsumori, M. Kiguchi, A. Maki, M. Abe, N. Tanaka, Extracting task-related activation components from optical

topography measurement using independent components analysis, J. Biomed. Opt. 13 (2008) 54008, https://doi.org/10.1117/1.2981829.
[70] R. Luke, M.J. Shader, D. McAlpine, Characterization of Mayer-wave oscillations in functional near-infrared spectroscopy using a physiologically informed model of the neural power spectra, Neurophotonics 8 (2021) 41001, https://doi.org/10.1117/1.NPh.8.4.041001.
[71] M.A. Yücel, J. Selb, C.M. Aasted, P.-Y. Lin, D. Borsook, L. Becerra, D.A. Boas, Mayer waves reduce the accuracy of estimated hemodynamic response functions in functional near-infrared spectroscopy, Biomed. Opt. Express 7 (2016) 3078–3088, https://doi.org/10.1364/BOE.7.003078.
[72] K.M. Spencer, J. Dien, E. Donchin, Spatiotemporal analysis of the late ERP responses to deviant stimuli, Psychophysiology 38 (2001) 343–358.
[73] G. Bauernfeind, S.C. Wriessnegger, S. Haumann, T. Lenarz, Cortical activation patterns to spatially presented pure tone stimuli with different intensities measured by functional near-infrared spectroscopy, Hum. Brain Mapp. 39 (2018) 2710–2724, https://doi.org/10.1002/hbm.24034.
[74] A.A. Stevens, P. Skudlarski, J.C. Gatenby, J.C. Gore, Event-related fMRI of auditory and visual oddball tasks, Magn. Reson. Imaging 18 (2000) 495–502, https://doi.org/10.1016/s0730-725x(00)00128-4.
[75] M. Tervaniemi, K. Hugdahl, Lateralization of auditory-cortex functions, Brain Res. Brain Res. Rev. 43 (2003) 231–246, https://doi.org/10.1016/j.brainresrev.2003.08.004.
[76] J. San Juan, X.-S. Hu, M. Issa, S. Bisconti, I. Kovelman, P. Kileny, G. Basura, Tinnitus alters resting state functional connectivity (RSFC) in human auditory and non-auditory brain regions as measured by functional near-infrared spectroscopy (fNIRS, PLoS One 12 (2017), e0179150, https://doi.org/10.1371/journal.pone.0179150.
[77] J. Saliba, H. Bortfeld, D.J. Levitin, J.S. Oghalai, Functional near-infrared spectroscopy for neuroimaging in cochlear implant recipients, Hear. Res. 338 (2016) 64–75, https://doi.org/10.1016/j.heares.2016.02.005.
[78] F. Mushtaq, I.M. Wiggins, P.T. Kitterick, C.A. Anderson, D.E.H. Hartley, The benefit of cross-modal reorganization on speech perception in pediatric cochlear implant recipients revealed using functional near-infrared spectroscopy, Front. Hum. Neurosci. 14 (2020) 308, https://doi.org/10.3389/fnhum.2020.00308.
[79] G.J. Basura, X.-S. Hu, J.S. Juan, A.-M. Tessier, I. Kovelman, Human central auditory plasticity: a review of functional near-infrared spectroscopy (fNIRS) to measure cochlear implant performance and tinnitus perception, Laryngoscope Investig. Otolaryngol. 3 (2018) 463–472, https://doi.org/10.1002/lio2.185.
[80] F. Mushtaq, I.M. Wiggins, P.T. Kitterick, C.A. Anderson, D.E.H. Hartley, Investigating cortical responses to noise-vocoded speech in children with normal hearing using functional near-infrared spectroscopy (fNIRS), J. Assoc. Res. Otolaryngol. 22 (2021) 703–717, https://doi.org/10.1007/s10162-021-00817-z.
[81] M.A. Yücel, A.V. Lühmann, F. Scholkmann, J. Gervain, I. Dan, H. Ayaz, D. Boas, R. J. Cooper, J. Culver, C.E. Elwell, A. Eggebrecht, M.A. Franceschini, C. Grova, F. Homae, F. Lesage, H. Obrig, I. Tachtsidis, S. Tak, Y. Tong, A. Torricelli, H. Wabnitz, M. Wolf, Best practices for fNIRS publications, Neurophotonics 8 (2021) 12101, https://doi.org/10.1117/1.NPh.8.1.012101.
[82] T. Funane, H. Atsumori, T. Katura, A.N. Obata, H. Sato, Y. Tanikawa, E. Okada, M. Kiguchi, Quantitative evaluation of deep and shallow tissue layers' contribution to fNIRS signal using multi-distance optodes and independent component analysis, Neuroimage 85 (Pt 1) (2014) 150–165, https://doi.org/10.1016/j.neuroimage.2013.02.026.
[83] K.-S. Hong, M.J. Khan, M.J. Hong, Feature extraction and classification methods for hybrid fNIRS-EEG brain-computer interfaces, Front. Hum. Neurosci. 12 (2018) 246, https://doi.org/10.3389/fnhum.2018.00246.
[84] A. von Lühmann, A. Ortega-Martinez, D.A. Boas, M.A. Yücel, Using the general linear model to improve performance in fNIRS single trial analysis and classification: a perspective, Front. Hum. Neurosci. 14 (2020) 30, https://doi.org/10.3389/fnhum.2020.00030.
[85] M.K. Yeung, V.W. Chu, Viewing neurovascular coupling through the lens of combined EEG-fNIRS: a systematic review of current methods, Psychophysiology 59 (2022), e14054, https://doi.org/10.1111/psyp.14054.
[86] S. Halder, M. Rea, R. Andreoni, F. Nijboer, E.M. Hammer, S.C. Kleih, N. Birbaumer, A. Kübler, An auditory oddball brain-computer interface for binary choices, Clin. Neurophysiol. J. Int. Fed. Clin. Neurophysiol. 121 (2010) 516–523, https://doi.org/10.1016/j.clinph.2009.11.087.
[87] G. Tortella, R. Casati, L.V.M. Aparicio, A. Mantovani, N. Senço, G. D'Urso, J. Brunelin, F. Guarienti, P.M.L. Selingardi, D. Muszkat, B. de, S.P. Junior, L. Valiengo, A.H. Moffa, M. Simis, L. Borrione, A.R. Brunoni, Transcranial direct current stimulation in psychiatric disorders, World J. Psychiatry 5 (2015) 88–102, https://doi.org/10.5498/wjp.v5.i1.88.